



## PAPER

# Spectral intensity of the N<sub>2</sub> emission in argon low-pressure arc discharges for lighting purposes

To cite this article: R Friedl and U Fantz 2012 *New J. Phys.* **14** 043016

View the [article online](#) for updates and enhancements.

## Related content

- [Diagnostics of low-pressure discharges containing InBr studied for lighting applications](#)  
S Briefi and U Fantz
- [Basics of plasma spectroscopy](#)  
U Fantz
- [Quantification of the VUV radiation in low pressure hydrogen and nitrogen plasmas](#)  
U Fantz, S Briefi, D Rauner et al.

## Recent citations

- [Two-phase Cryogenic Avalanche Detector with electroluminescence gap operated in argon doped with nitrogen](#)  
A. Bondar *et al*
- [Photon emission and atomic collision processes in two-phase argon doped with xenon and nitrogen](#)  
A. Buzulutskov
- [Intricate Plasma-Scattered Images and Spectra of Focused Femtosecond Laser Pulses](#)  
C. H. Raymond Ooi and Md. Ridzuan Talib

## Spectral intensity of the N<sub>2</sub> emission in argon low-pressure arc discharges for lighting purposes

R Friedl<sup>1,2,3</sup> and U Fantz<sup>1,2</sup>

<sup>1</sup> Lehrstuhl für Experimentelle Plasmaphysik, Universität Augsburg,  
Universitätsstrasse 1, 86135 Augsburg, Germany

<sup>2</sup> Max-Planck-Institut für Plasmaphysik, EURATOM Association,  
Boltzmannstrasse 2, 85748 Garching, Germany  
E-mail: [roland.friedl@physik.uni-augsburg.de](mailto:roland.friedl@physik.uni-augsburg.de)

*New Journal of Physics* **14** (2012) 043016 (22pp)

Received 19 September 2011

Published 17 April 2012

Online at <http://www.njp.org/>

doi:10.1088/1367-2630/14/4/043016

**Abstract.** Nitrogen is discussed as an alternative to hazardous mercury in lamps for general lighting. Molecular nitrogen bands emit in both the near-UV (the second positive system  $C^3\Pi_u \rightarrow B^3\Pi_g$ ) and the visible spectral range (the first positive system  $B^3\Pi_g \rightarrow A^3\Sigma_u^+$ ), which reduces conversion losses. To analyse the potential of nitrogen, low-pressure arc discharges in an argon background were characterized by means of optical emission spectroscopy. The spectral intensity of the molecular nitrogen emission rises with increasing nitrogen content in the discharge and shows a maximum around 4 mbar of absolute pressure. With regard to the application as a light source, radiation efficiencies were determined, which are around 5% at maximum. In order to identify the main population processes a collisional radiative model for the nitrogen–argon system was established which reveals the high relevance of heavy-particle collisions due to a pressure of a few mbar. The decisive excitation reactions for the state  $N_2 C^3\Pi_u$  are the well-known processes of energy pooling between metastable nitrogen molecules and energy transfer from metastable argon atoms. For the state  $N_2 B^3\Pi_g$  the main population channels are collision-induced crossings within the nitrogen states, where the collision partner can be either a nitrogen molecule or an argon atom, and the quenching collisions with argon.

<sup>3</sup> Author to whom any correspondence should be addressed.

**Contents**

<b>1. Introduction</b>	<b>2</b>
<b>2. Experiment</b>	<b>3</b>
2.1. Experimental setup . . . . .	3
2.2. Diagnostic of plasma parameters . . . . .	4
<b>3. Collisional radiative model for the nitrogen–argon system</b>	<b>7</b>
3.1. Energy levels . . . . .	7
3.2. Reactions . . . . .	8
<b>4. Results</b>	<b>12</b>
4.1. Measured emission properties . . . . .	12
4.2. Comparison with collisional radiative modelling . . . . .	13
4.3. Radiation efficiencies and variation of the discharge current . . . . .	18
<b>5. Conclusions</b>	<b>20</b>
<b>Acknowledgments</b>	<b>21</b>
<b>References</b>	<b>21</b>

**1. Introduction**

Conventional fluorescent lamps use mercury as an ultraviolet (UV) emitter at 254 nm and convert this emission via phosphors into the visible (VIS) spectral range. The disadvantages of this method of producing VIS light include the toxicity of mercury and the high energy loss owing to conversion. Therefore, mercury-free discharge lamps are a prevailing issue in current research [1–3]. In mercury-based lamps, UV emission is very efficient due to the underlying resonant transition and the existence of six isotopes with noticeable natural abundances, where each of them has slightly different emission lines, which leads to a low optical depth. No other element reaches comparable efficiencies even when taking conversion losses into account. Therefore, molecules are discussed, for instance, as emitting substances [4].

Nitrogen, an environment-friendly, chemically inert and almost unlimitedly available gas, is a promising candidate as an alternative emitter. Its prominent emission systems, the first positive system ( $B^3\Pi_g \rightarrow A^3\Sigma_u^+$ ) and the second positive system ( $C^3\Pi_u \rightarrow B^3\Pi_g$ ), are useful for lighting applications. While the B–A transition emits from the VIS to the near-infrared (near-IR, 500–2500 nm), the C–B emission arises in the near-UV spectral range (260–430 nm). Therefore, the main advantages of using nitrogen as the emitter are lower conversion losses and the possibility of directly using VIS light. Furthermore, gaseous nitrogen has a temperature-independent emission as compared to liquid mercury and offers an opportunity for the direct substitution of mercury in lamp fabrication. First investigations on nitrogen-based discharge lamps are presented in [5] and [6], where different excitation methods (internal/external electrodes, tesla coil and dc glow discharge) were used. These results show, in principle, the applicability of nitrogen molecular emission as an alternative to mercury in lamps for general lighting. However, the pursued methods for plasma generation would require fundamental modifications in lamp design as conventional fluorescent lamps with mercury are low-pressure arc discharges.

This paper is devoted to the investigation of low-pressure arc discharges in nitrogen and nitrogen–argon mixtures. A characterization of the discharge is presented regarding the

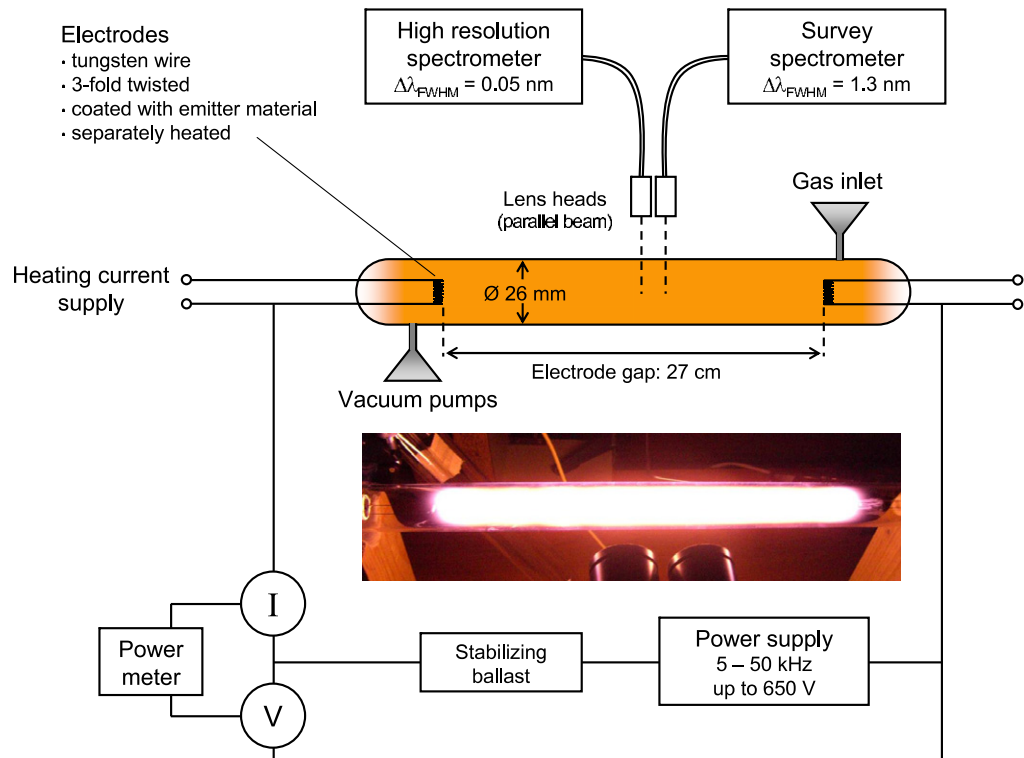


**Figure 1.** Experimental setup of the discharge with the diagnostics.

emission properties and their dependence on the plasma parameters. A non-rotationally resolved collisional radiative model (CR model), which couples molecular nitrogen and argon, is constructed in order to identify the relevant population mechanisms in the investigated parameter range. The CR model is validated in nitrogen by comparing it to emission measurements and can be used for systematic plasma parameter studies. With regard to application as a light source, the radiation efficiencies depending on the absolute pressure and the nitrogen content in the argon background are determined and compared to conventional fluorescent lamps.

## 2. Experiment

### 2.1. Experimental setup

The basic setup is shown in figure 1 and is designed similar to conventional fluorescent lamps, i.e. the discharge vessel has tube geometry (26 mm in diameter) and electrical power is supplied to the discharge via internal electrodes (electrode gap 27 cm). The vessel is integrated in a vacuum system to provide a wide accessible parameter space of pressure and nitrogen concentrations in different rare gases as the background. Absolute pressures are measured with a capacitive pressure gauge (Baratron), whereas the mixture is regulated by mass flow controllers. The electrodes consist of a threefold twisted tungsten wire, which is coated with emitter material and can be heated separately. The power supply generates ac voltages up to 650 V at frequencies

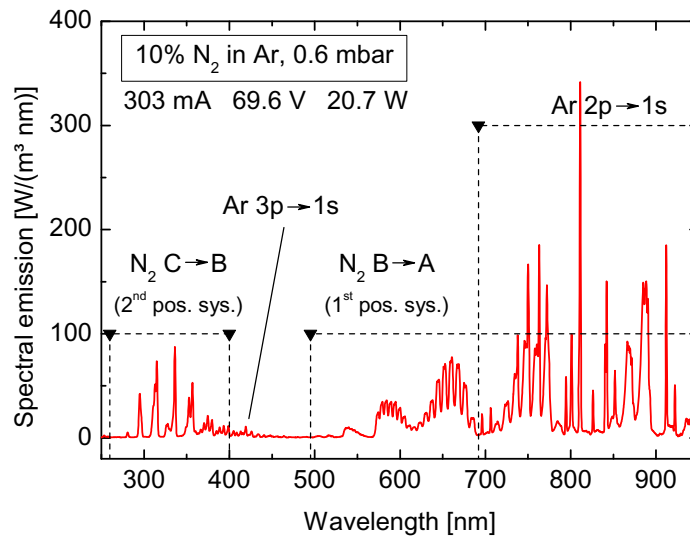


**Figure 2.** Typical spectrum of nitrogen–argon arc discharges with designated parts of the emission.

from 5 to 50 kHz (so far driven at 20 kHz). A stabilizing ballast is used for current limiting purposes. For diagnostics, the electrical parameters, namely the discharge current  $I$ , the voltage  $U$  and the power  $P_{\text{el}}$ , are recorded by a power meter. For the optical emission spectroscopy, centred radial lines of sight are used with a diameter of 1 cm. A survey spectrometer and a high-resolution spectrometer with Gaussian apparatus profiles of  $\Delta\lambda_{\text{FWHM}} = 1.3$  and 0.05 nm, respectively, are applied. Calibration is done using an Ulbricht sphere and a deuterium arc lamp. Stable and reproducible arc discharges can be generated in gas mixtures of 0.1% nitrogen in argon up to pure nitrogen, absolute pressures between  $10^{-1}$  and  $10^2$  mbar and discharge currents of 100–500 mA.

Figure 2 shows a characteristic emission spectrum from a  $\text{N}_2$ –Ar plasma in the present experimental setup. Such an arc discharge has intense emission from the first and the second positive systems of molecular nitrogen covering broad emission in the near-UV, the VIS and the near-IR spectral range. Radiation from the molecular ion such as the first negative system is strongly overlapped by the second positive system and not identifiable in the spectrum, whereas emission from atomic nitrogen is not detectable. The nitrogen radiation is accompanied by emission resulting from the  $2p \rightarrow 1s$  transitions of the argon atom. The spectral gap between the two nitrogen systems (400–550 nm) should then be closed by the use of phosphors which convert the near-UV emission from the  $\text{N}_2$  C–B transition while being virtually transparent for the B–A system. The combination of converted UV emission with the VIS radiation from the first positive system demonstrates the possibility of using nitrogen low-pressure arc discharges as light sources.

## 2.2. Diagnostic of plasma parameters

### 2.2.1. Gas temperature.

Determination of particle densities from the measured pressures via the ideal gas law requires knowledge of the gas temperature. For nitrogen a well-established diagnostic for  $T_{\text{gas}}$  exists by means of the rotational temperature of the bands of

the second positive system of  $N_2$  or the first negative system of the molecular ion  $N_2^+$  [7, 8]. In the present discharge, this technique cannot be employed due to the high absolute pressures and the usage of gas mixtures with an argon background, which leads to the dominance of heavy-particle collisions for the excitation of the C state of nitrogen (see section 4.2). Accordingly, the correlation between the rotational temperature of the excited C state and the gas temperature is distorted [7, 9]. Secondly, these population channels lead to intense emission from the second positive system whose bands are superimposed on the bands of the molecular ion. Hence, the first negative system of nitrogen cannot be evaluated either in the present arc discharge. Therefore the gas temperature can only be estimated by using the relation  $T_{\text{ambient}} \leq T_{\text{gas}} \leq T_{\text{rot}}$ . Rotational temperatures were determined by adjusting simulated to measured spectra with  $T_{\text{rot}}$  as parameter [8]. Using the experimentally specified rotational temperatures of about 1000 K, the gas temperature is assumed to be  $700 \pm 300$  K. This uncertainty affects the analysis of further plasma parameters via the undetermined ground state density  $n_0$ , as will be discussed for  $n_e$  and  $T_e$ .

*2.2.2. Electron density.* Due to the lack of diagnostic ports at the quartz vessel, conventional electrical probe measurements for the determination of the plasma parameters cannot be applied to the present setup. The use of a microwave interferometer, on the other hand, is limited by the small radial dimension of the discharge tube. In addition, it requires a free accessible axial line of sight, which cannot be provided due to the electrodes. Optical methods using the emission of specific argon neutral lines [8] or ion lines [10] fail since the required argon lines are overlapped by nitrogen bands and ion lines are not detectable.

A convenient and non-disturbing method, however, is to determine the electron density  $n_e$  from the discharge current  $I$  via the relation

$$I = A \cdot |j| = A \cdot e \cdot n_e \cdot v_D \left( \frac{E}{n_0} \right), \quad (1)$$

where  $A$  is the cross-sectional area of the arc discharge,  $j$  is the discharge current density,  $e$  is the elementary charge and  $v_D$  is the drift velocity of the electrons depending on the accelerating electrical field  $E$  in a gas of density  $n_0$ . For the investigated gas mixtures of argon and nitrogen, experimentally determined drift velocities depending on the reduced electrical field  $E/n_0$  were taken from the literature. Values for the pure gases were collected from several references and combined using a least squares fit (for argon from [11–15] and for nitrogen from [13, 15]). For  $N_2$ -Ar mixtures, there are recently measured data in [16], and moreover, in [17] an empirical formula is evaluated with which the drift velocities in  $N_2$ -Ar mixtures can be calculated depending on the nitrogen content. These calculated values are consistent with the measurements in [16] for the relevant range of  $E/n_0$  of the present discharge. Hence, the formula in [17] can be used for mixtures where no drift velocity measurements exist in the literature.

The electrical field  $E$  was determined by dividing the discharge voltage  $U$  by the electrode gap  $d$  neglecting the cathode fall voltage. As there is a clearly observable hot spot at the electrodes in the present arc discharges, thermal emission of electrons dominates over secondary electron emission by ion bombardment. Therefore, the cathode fall plays only a minor role compared to glow discharges, for which reason the simplification of neglecting this voltage drop is applicable to a certain extent. Due to the characteristic of an arc discharge the cathode fall voltage can be assumed to be connected to the ionization energy of the containing gases,

which is about 16 eV in the present case. Reducing the adopted voltage by these 16 V, the actual electrical field and therefore the electron drift velocity in the discharge are lower, which results in the evaluation of a higher electron density. In relation to the discharge voltage, which is between  $\approx 30$  and 250 V for the investigated parameter space, the neglect of the cathode fall voltage could lead to an underestimation of the determined electron density of up to 60%. This deviation is lower at higher discharge voltages and therefore lower for higher contents of nitrogen in the discharge and higher absolute pressures. Another source of error for  $n_e$  is the required neutral gas density  $n_0$ , which is undetermined due to the mentioned lack of diagnostics for the gas temperature. These two effects lead to an uncertainty in  $n_e$  between  $-30$  and  $+100\%$  at maximum.

**2.2.3. Electron temperature.** Since Langmuir probes are not available in the present setup, measurements of the electron energy distribution function (EEDF) are not possible. Therefore as a first approach an electron temperature  $T_e$  is used that characterizes the EEDF as Maxwellian. The electron temperature can be determined by optical emission spectroscopy using the line emission  $I_{ik}$  from an optical transition  $i \rightarrow k$  [10]:

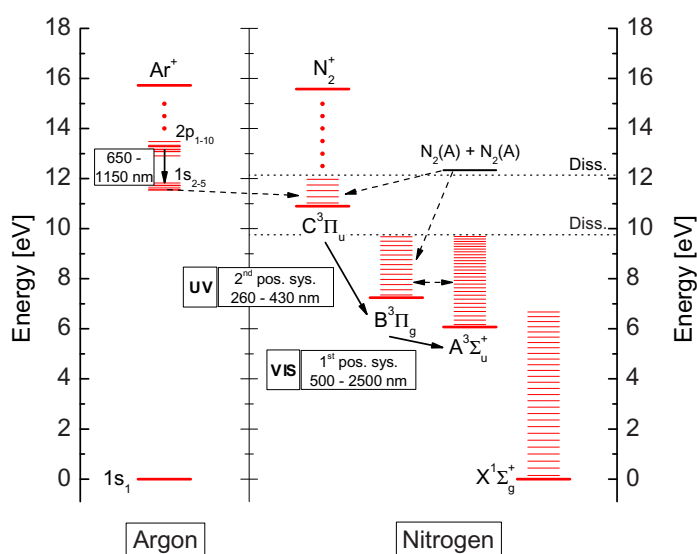
$$I_{ik} = n_0 \cdot n_e \cdot X_{\text{Em},ik}^{\text{eff}}(T_e, n_e, \dots), \quad (2)$$

where  $X_{\text{Em},ik}^{\text{eff}}$  is the effective emission rate coefficient. Appropriate and undisturbed lines of the background gas argon can be analysed for this purpose. The corresponding effective rate coefficients have to be calculated with a CR model, of which there are several available in the literature for the argon atom [18–22]. For the present investigations, the CR model Yacora [23] is applied, since this solver is also used for nitrogen (see section 3.2) and allows for easy coupling to other species that are important for heavy-particle collisions. The solver Yacora balances a set of excitation and de-excitation channels for the excited states of the argon atom [24]: detailed balanced electron collision processes as well as optical transitions between the ground state and the  $1s_{2-5}$  and  $2p_{1-10}$  excited states (Paschen notation), electron impact ionization from the  $1s$  and  $2p$  states, Penning ionization by metastable  $1s$  states, electron quenching of the  $1s$  states and diffusion of the  $1s$  metastables to the wall as well as opacity of the resonance lines. For the validation of this CR model, a systematic literature review was conducted for the input data and the modeling results were consistently compared to measurements by means of optical emission and absorption spectroscopy and a Langmuir probe [24]. Taking into account the interaction with nitrogen molecules in the present discharge, excitation transfer from the argon  $1s$  metastable states to the C state of nitrogen is adopted as an additional loss mechanism for Ar metastables (see reaction (18) in table 2).

Several argon lines were used for the determination of  $T_e$  in order to eliminate errors arising from interfering nitrogen bands. The evaluated transitions together with the transition probabilities  $A_{ik}$  and the line branching ratios ( $A_{ik}/\sum_l A_{il}$ ) are summarized in table 1. The particular determined electron temperatures of the analysed lines were subsequently averaged, a typical standard deviation being 0.04 eV in the investigated temperature range of 1–3 eV. The main sources of error in the determination of  $T_e$  are the uncertainties in electron and neutral gas density. Thus, for electron temperatures close to 3 eV (low pressure), the error in  $T_e$  is  $-0.6$  eV and  $+0.4$  eV, whereas close to 1 eV (high pressure) the error reduces to  $\pm 0.05$  eV.

**Table 1.** Characteristics of the argon lines [25] used for determining the electron temperature.

Wavelength (nm)	Transition	$A_{ik}$	Branching ratio
696.5	$2p_2 \rightarrow 1s_5$	$6.4 \times 10^6 \text{ s}^{-1}$	0.18
706.7	$2p_3 \rightarrow 1s_5$	$3.8 \times 10^6 \text{ s}^{-1}$	0.11
750.4	$2p_1 \rightarrow 1s_2$	$4.5 \times 10^7 \text{ s}^{-1}$	0.99
751.5	$2p_5 \rightarrow 1s_4$	$4.0 \times 10^7 \text{ s}^{-1}$	1.00
811.5	$2p_9 \rightarrow 1s_5$	$3.3 \times 10^7 \text{ s}^{-1}$	1.00

**Figure 3.** Relevant energy levels for argon [25] and molecular nitrogen [26] including vibrational states for  $N_2$ , ionization and dissociation energies, prominent optical transitions (solid arrows) and heavy-particle reactions (dashed arrows). The level named ' $N_2(A) + N_2(A)$ ' illustrates the minimal energy level for two colliding metastable nitrogen molecules.

### 3. Collisional radiative model for the nitrogen–argon system

#### 3.1. Energy levels

Figure 3 illustrates energy levels of argon and molecular nitrogen which are relevant for the present investigations. For argon, the  $1s$  and the  $2p$  states (Paschen notation) are of interest as the emission lines between 650 and 1150 nm arise from the transitions  $2p_x \rightarrow 1s_y$ . Levels  $1s_5$  and  $1s_3$  are metastable, whereas  $1s_4$  and  $1s_2$  are resonant states, i.e. radiation to the ground state is allowed. In nitrogen, the prominent emission systems (the first and the second positive system) occur due to electronic transitions between the ro-vibrational levels of the triplet states  $C^3\Pi_u$ ,  $B^3\Pi_g$  and  $A^3\Sigma_u^+$ , whereas the A state is metastable. For clarity, rotational levels are not shown in figure 3. The electronic states B and C pre-dissociate for vibrational quantum numbers  $\nu_B > 12$



and  $\nu_C > 4$ , which correspond to 9.8 and 12.1 eV, respectively [26]. The ionization energy for both gases is very similar, 15.7 eV for argon and 15.6 eV for molecular nitrogen.

Well-known heavy-particle collisions like energy transfer from metastable argon into the C state of nitrogen or energy pooling reactions within the nitrogen states are indicated as dashed arrows in figure 3 and will be described in detail in the next section.

### 3.2. Reactions

A CR model for the electronic states  $X^1\Sigma_g^+$ ,  $A^3\Sigma_u^+$ ,  $B^3\Pi_g$  and  $C^3\Pi_u$  of nitrogen was established in order to simulate the emission of the first and the second positive systems in the present arc discharge. In a first approach, this model was chosen to be neither rotationally nor vibrationally resolved, as only the integral emission and the separation into UV and VIS radiation was of interest together with the coupling to the electronic states of the argon atom. The spectral ro-vibrationally distribution, however, is of minor interest for this study, whereas it has been extensively studied, for example, in [27, 32, 39, 40, 42–51]. Therefore the emission from both the nitrogen systems is to be seen as an integral over all vibrational bands (in simulation as well as experimentally).

Models for molecular nitrogen are widely used [27–32], whereas the extensive studies by the group of Ferreira, Loureiro and Guerra on nitrogen glow discharges (e.g. [30, 52]) and the investigations on nitrogen heavy-particle collisions by Piper (e.g. [39, 40, 43, 46]) are used as the basis for the current model because of the comparability of experimental parameters with the present setup, in particular the pressure range. Electron collision processes, spontaneous emission, diffusion and heavy-particle collisions were taken into account for calculating the population density of the aforementioned triplet states. The model is restricted to the states X, A, B and C, whereas at present, cascade processes from energetically higher-lying electronic states are not taken into account and optical depth is neglected due to the small discharge diameter.

The processes implemented in the CR model are summarized in table 2 together with the respective rate coefficients. The listed values for  $k$  are given as non-vibrationally resolved rate coefficients in the corresponding references with the exception of reaction (20), which is discussed in detail in section 3.2.4.

**3.2.1. Electron impact processes.** For the electron collisions (1)–(8) impact cross sections  $\sigma(E)$  are used ([33–35]; for (7), (8) shifted according to threshold energies) which are convolved with a Maxwellian EEDF, whereas processes (1)–(3) are evaluated by detailed balancing.

**3.2.2. Spontaneous emission.** Vibrationally resolved transition probabilities  $A_{BA}^{v'v''}$  and  $A_{CB}^{v'v''}$  for the first and the second positive system of nitrogen (reactions (9) and (10)) are given in [36]. Since the model is not vibrationally resolved, effective Einstein coefficients  $A^{\text{eff}}$  have to be used that take the vibrational population of the C and the B states into account. The latter are deduced from the spectroscopic measurements (see section 4.2).  $A^{\text{eff}}$  is then calculated by the weighted sum of the vibronic transition probabilities [37]. Since the measurements showed only a minor dependence of the relative vibrational populations on the discharge parameters, the effective transition probabilities for both nitrogen systems are adopted as constants in the model.

**3.2.3. Diffusion.** The diffusion of metastable nitrogen molecules  $A^3\Sigma_u^+$  (reaction (11)) is characterized by the diffusion time  $\tau_{\text{diff}}(p, T_{\text{gas}})$ , which is parameterized after [38]. Since the

**Table 2.** Considered processes in the CR model for the nitrogen–argon system including the corresponding rate coefficients. In processes (16) and (17), M stands for either ( $M = \text{N}_2$ ) or ( $M = \text{N}_2 + \text{Ar}$ ) as discussed in the text.

Reaction	Rate coefficient	Reference
Electron impact excitation and de-excitation:		
(1) $e + \text{N}_2(\text{X}) \leftrightarrow \text{N}_2(\text{A}) + e$	Convolved $\sigma(E)$	[33]
(2) $e + \text{N}_2(\text{X}) \leftrightarrow \text{N}_2(\text{B}) + e$	Convolved $\sigma(E)$	[33]
(3) $e + \text{N}_2(\text{X}) \leftrightarrow \text{N}_2(\text{C}) + e$	Convolved $\sigma(E)$	[33]
(4) $e + \text{N}_2(\text{A}) \rightarrow \text{N}_2(\text{B}) + e$	Convolved $\sigma(E)$	[34]
Electron impact ionization:		
(5) $e + \text{N}_2(\text{X}) \rightarrow \text{N}_2^+ + 2e$	Convolved $\sigma(E)$	[35]
(6) $e + \text{N}_2(\text{A}) \rightarrow \text{N}_2^+ + 2e$	Convolved $\sigma(E)$	[35]
(7) $e + \text{N}_2(\text{B}) \rightarrow \text{N}_2^+ + 2e$	Convolved $\sigma_{(6)}(E - 1.18 \text{ eV})$	
(8) $e + \text{N}_2(\text{C}) \rightarrow \text{N}_2^+ + 2e$	Convolved $\sigma_{(6)}(E - 4.86 \text{ eV})$	
Spontaneous emission:		
(9) $\text{N}_2(\text{B}) \rightarrow \text{N}_2(\text{A}) + h\nu$	$A^{\text{eff}} = 1.2 \times 10^5 \text{ s}^{-1}$	$A_{\text{BA}}^{v'v''}$ from [36]
(10) $\text{N}_2(\text{C}) \rightarrow \text{N}_2(\text{B}) + h\nu$	$A^{\text{eff}} = 2.6 \times 10^7 \text{ s}^{-1}$	$A_{\text{CB}}^{v'v''}$ from [36]
Diffusion:		
(11) $\text{N}_2(\text{A}) + \text{wall} \rightarrow \text{N}_2(\text{X})$	$\tau_{\text{diff}}(p, T_{\text{gas}})$ parameterized after [38]	
Energy pooling:		
(12) $\text{N}_2(\text{A}) + \text{N}_2(\text{A}) \rightarrow \text{N}_2(\text{B}) + \text{N}_2(\text{X})$	$k = 7.7 \times 10^{-17} \text{ m}^3 \text{ s}^{-1}$	[39]
(13) $\text{N}_2(\text{A}) + \text{N}_2(\text{A}) \rightarrow \text{N}_2(\text{C}) + \text{N}_2(\text{X})$	$k = 1.5 \times 10^{-16} \text{ m}^3 \text{ s}^{-1}$	[40]
Quenching:		
(14) $\text{N}_2(\text{B}) + \text{N}_2(\text{X}) \rightarrow \text{N}_2(\text{X}) + \text{N}_2(\text{X})$	$k = 1.5 \times 10^{-18} \text{ m}^3 \text{ s}^{-1}$	[30]
(15) $\text{N}_2(\text{C}) + \text{N}_2(\text{X}) \rightarrow \text{N}_2(\text{X}) + \text{N}_2(\text{X})$	$k = 7.1 \times 10^{-18} \text{ m}^3 \text{ s}^{-1}$	[41]
Collision-induced transition:		
(16) $\text{N}_2(\text{A}) + \text{M} \rightarrow \text{N}_2(\text{B}) + \text{M}$	$k = 2.0 \times 10^{-17} \text{ m}^3 \text{ s}^{-1}$	[30] see discussion
(17) $\text{N}_2(\text{B}) + \text{M} \rightarrow \text{N}_2(\text{A}) + \text{M}$	$k = 2.85 \times 10^{-17} \text{ m}^3 \text{ s}^{-1}$	[30] see discussion
Excitation transfer:		
(18) $\text{Ar}_{\text{meta}}^* + \text{N}_2(\text{X}) \rightarrow \text{Ar} + \text{N}_2(\text{C})$	$k = 3.2 \times 10^{-17} \text{ m}^3 \text{ s}^{-1}$	[42]
Quenching:		
(19) $\text{N}_2(\text{A}) + \text{N} \rightarrow \text{N}_2(\text{X}) + \text{N}$	$k = 4 \times 10^{-17} \text{ m}^3 \text{ s}^{-1}$	[43]
(20) $\text{N}_2(\text{B}) + \text{Ar} \rightarrow \text{N}_2(\text{X}) + \text{Ar}$	$k^{\text{eff}} = 10^{-19} \text{ m}^3 \text{ s}^{-1}$	$k^{v'}$ from [44]
Recombination:		
(21) $\text{N} + \text{N} + \text{N}_2(\text{X}) \rightarrow \text{N}_2(\text{B}) + \text{N}_2(\text{X})$	$k = 4 \times 10^{-45} \text{ m}^6 \text{ s}^{-1}$	[45]
(22) $\text{N} + \text{N} + \text{Ar} \rightarrow \text{N}_2(\text{B}) + \text{Ar}$	$k = 4 \times 10^{-45} \text{ m}^6 \text{ s}^{-1}$	[45]

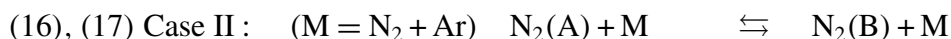
discharge operates in the intermediate range of ‘normal’ and ‘free fall’ diffusion the respective diffusion times for the confinement of neutrals are added. These depend on the absolute pressure, the gas temperature, the masses of the collision partners, the collisional cross section, the mean diffusion length and the characteristic linear dimension. The latter two lengths are determined by experimental dimensions and the collisional cross section is approximated by the hard-sphere model reflecting the diffusion of nitrogen molecules in argon. The values used are given in table 3.

**Table 3.** Parameters for calculating the diffusion time  $\tau_{\text{diff}}$  for reaction (11).

Parameter	Value
Mean diffusion length	0.0054 m
Characteristic linear dimension	0.0065 m
Collisional cross section	$4.7 \times 10^{-19} \text{ m}^2$

**3.2.4. Interactions with argon.** The background gas argon affects the population of the nitrogen states, which has to be taken into account. For the C state, excitation transfer from metastable argon atoms (18) is a well-known population channel in nitrogen–argon plasmas. The rate coefficient for this reaction is taken from extensive investigations by the group of Vredenburg [42]. For the B state, quenching by argon atoms (20) and atom recombination of nitrogen via argon (22) influence the population density, in particular at high pressures [44, 45]. The effective rate coefficient  $k^{\text{eff}}$  for reaction (20) was calculated using the vibrationally resolved coefficients  $k^{v'}$  given in [44], which were summed up weighted according to experimentally determined relative population densities of the vibrational B states (see section 4.2). According to the minor dependence of the relative vibrational population on the discharge parameters, again a constant value for  $k^{\text{eff}}$  was used. The consequences of this simplification will be discussed in section 4.2.2.

**3.2.5. Transitions between the states A and B.** A crucial point is the processes involving transitions between the A and B states of nitrogen (16) and (17). In the literature there is no direct consensus about the actual nature of these reactions [46–51]. The collision partner M can be treated either as nitrogen only (case I) or as both nitrogen and argon (case II):



If these reactions took place as excitation transfer processes from one molecule ( $\text{N}_2$ ) to another ( $\text{N}'_2$ ), obviously only case I could be possible. Case II would be the matter for a collision-induced crossing within one nitrogen molecule. In other words, the question is whether or not argon can induce the transition from the A to the B state in nitrogen, as for pure nitrogen both alternatives are equivalent when calculating the population density of the B state.

Case I is regarded as the correct perception by Piper [46]. It is argued that the Franck–Condon factors for the transitions  $(\text{X}, v'') \rightarrow (\text{B}, v')$  are much greater than those for  $(\text{A}, v'') \rightarrow (\text{B}, v')$ . This would be indicative of an exchange of energy from one molecule in the A state to another molecule which is thereby excited from the ground state to the B state. The energy transfer formalism is also favoured in a paper by Privilov *et al* [47] in which this issue is circumstantiated by using isotopically labelled nitrogen. Via the shift in the positions of the band heads of the first positive system, they have apparently proven that ground state molecules  $^{14}\text{N}_2(\text{X})$  were excited in collisions with  $^{15}\text{N}_2(\text{B}, \text{A})$ .

Nevertheless, neither Piper nor Privilov [46, 47] investigated nitrogen discharges with background gases. Campbell and Thrush [48], however, studied the partial replacement of nitrogen by argon in their investigations on the nitrogen afterglow phenomenon, which is attributed to the first positive system. To explain the emergence of the afterglow emission

they suggested a collision-induced transition from the metastable A state to the emitting B state. For their explanations they treated nitrogen and argon as equivalent collision partners, which corresponds to case II for the processes (16) and (17). In a subsequent paper [49], they investigated especially the kinetics of  $N_2$   $B^3\Pi_g$  and found comparable efficiencies for argon and nitrogen in inducing the crossing processes  $A \rightleftharpoons B$ . Furthermore, they determined rate coefficients for these transitions claiming equal rates for both directions. However, Carlson *et al* [50] evaluated a rate coefficient roughly three orders of magnitude larger than that of Gartner and Thrush [49] (but again the same for nitrogen and argon). In addition, they remarked that several states might be suitable precursors for collisional transfer to  $N_2$   $B^3\Pi_g$ , namely  $A^3\Sigma_u^+$ ,  $W^3\Delta_u$ ,  $B'^3\Sigma_u^-$ ,  $a'^1\Sigma_u^-$ ,  $a^1\Pi_g$  and/or  $^5\Sigma_g^+$ . The latest publication known to the authors is the paper by Bachmann *et al* [51]. Besides the explanation of enhanced nitrogen afterglow by collisional transition from the A to the B state induced by all rare gases and various diatomic molecules, they determined relative cross sections for the different collision partners revealing approximately equal values for nitrogen and argon.

Taking this survey into account, i.e. (i) the general possibility of collision-induced crossing between the nitrogen states by third bodies such as argon [48–51], (ii) the almost equal efficiency of nitrogen and argon in inducing the transition [49–51] and (iii) the approximate equilibrium of both directions of the collisional crossing  $A \rightleftharpoons B$  [49], processes (16) and (17) can obviously be considered to have either a nitrogen molecule or an argon atom as the collision partner (case II).

In order to account for the presented disagreement in the literature and in order to show the significance of different approaches for reactions (16) and (17), both cases were considered as options in the calculations. The rate coefficients for nitrogen as a collision partner were taken from Guerra and Loureiro [30]. For case II these rate coefficients were also taken for argon according to assumptions (ii) and (iii).

**3.2.6. Emission of the nitrogen band systems.** Using the excitation and de-excitation channels listed in table 2, the nonlinear solver Yacora [23] solves the coupled system of rate equations and calculates the absolute densities of the electronic states  $A^3\Sigma_u^+$ ,  $B^3\Pi_g$  and  $C^3\Pi_u$  of nitrogen. The emission from the first and the second positive system is then obtained by simply multiplying the densities with the appropriate effective transition probabilities  $A^{\text{eff}}$ .

Input parameters for the CR calculations are as follows:

- plasma parameters  $n_e$  and  $T_e$  as they are determined experimentally (see section 2.2);
- absolute pressure  $p$  as measured and gas temperature  $T_{\text{gas}}$  that is assumed to be 700 K (see section 2.2);
- densities of molecular nitrogen  $n_{N_2}$  and argon  $n_{Ar}$  in the ground state as deduced from the partial pressures;
- density of atomic nitrogen  $n_N$  (a dissociation degree of 3% is assumed which is reasonable from a comparison to experiments with similar discharge parameters [30, 31, 44, 45, 52]);
- density of metastable argon atoms  $n_{Ar^*_{\text{meta}}}$  as calculated with the CR model Yacora argon [24] using the appropriate input parameters  $n_e$ ,  $T_e$ ,  $T_{\text{gas}}$ ,  $p$ ,  $n_{Ar}$  and  $n_{N_2}$ .

Uncertainties of the input parameters (which are mostly attributed to the unknown  $T_{\text{gas}}$ ) were taken into account by performing calculations with the maximal and minimal values of the particular parameters. This is also applied for the CR calculation of  $n_{Ar^*_{\text{meta}}}$ . The results of these sensitivity studies are shown and discussed in section 4.2.

## 4. Results

### 4.1. Measured emission properties

The spectra of nitrogen–argon low-pressure arc discharges vary strongly with nitrogen content and absolute pressure. Within the limits of the investigated parameter range, nitrogen-dominated spectra as well as argon-dominated spectra can be observed. A spectrum in which the radiation of both gases can be seen clearly is shown in figure 2. For the analysis of the emission, the following line integrals were examined in particular. The second positive system of nitrogen can be observed entirely within the integral limits from 260 to 400 nm. In addition, the emission is not disturbed by  $N_2^+$  emission or argon lines. For the first positive system, many argon lines interfere with the nitrogen bands and emission above 950 nm cannot be recorded with the present spectroscopic setup. Therefore representative emission bands between 495 and 691 nm were integrated corresponding to the vibrational sequences  $\Delta v = +3, \dots, +6$ . According to the vibrational population and the transition probabilities, these sequences account for approximately 15–25% of the whole emission from this system. The precise value depends on nitrogen content and absolute pressure. This accuracy is regarded to be sufficient, as no differences are expected between the behaviour of these sequences and the whole system. In addition, this integral is more representative of the application of  $N_2$  as a light source as it is confined to the VIS spectral range. The argon emission is monitored using the line emission at 811.5 nm (transition  $2p_9 \rightarrow 1s_5$ ), which is the strongest line in each spectrum that is not superimposed by nitrogen emission.

Figure 4 shows the dependence of the emission intensities, i.e. the two representative nitrogen systems and the argon line emission, on the concentration of nitrogen in argon for 1 mbar absolute pressure. The corresponding plasma parameters are derived according to section 2.2. In the case of pure nitrogen where no argon lines are available,  $T_e$  was evaluated using the CR model Yacora nitrogen, as will be discussed in section 4.2.1. The electron drift velocity in nitrogen discharges is higher than in argon discharges. This leads to a declining electron density with rising nitrogen content when the discharge current is kept constant at 300 mA (see equation (1)). In contrast, the electron temperature remains constant when varying the gas mixture in accordance with the ionization balance [8] (similar ionization energies). The emission from the argon line decreases due to the strong decrease of  $n_e$  and the small reduction of the argon density with increasing nitrogen content. The increase in the nitrogen emission is determined by the increasing molecular density compensating the decreasing  $n_e$ .

In figure 5, the pressure dependence of the nitrogen and argon emission and of the plasma parameters is presented for 1% nitrogen in argon. For sustaining the discharge current at 300 mA, a rising  $n_e$  is required when the pressure is raised due to the declining electron drift velocity through the higher gas density. Simultaneously, the electron temperature decreases as expected according to the ionization balance [8], i.e. the ion confinement time increases due to the reduced diffusion. These contrary trends of  $n_e$  and  $T_e$  yield a maximal nitrogen emission in the mid-pressure range. The argon emission, however, shows a strong dependence on pressure. This can be attributed to the decreasing electron temperature to which the argon emission is more sensitive than the nitrogen emission as the energy threshold for argon is about 13 eV compared to 11 and 7 eV in nitrogen.

Comparing the spectra of discharges with different nitrogen contents and absolute pressures, it can be summarized that above a nitrogen concentration of 5% (at 1 mbar) or an

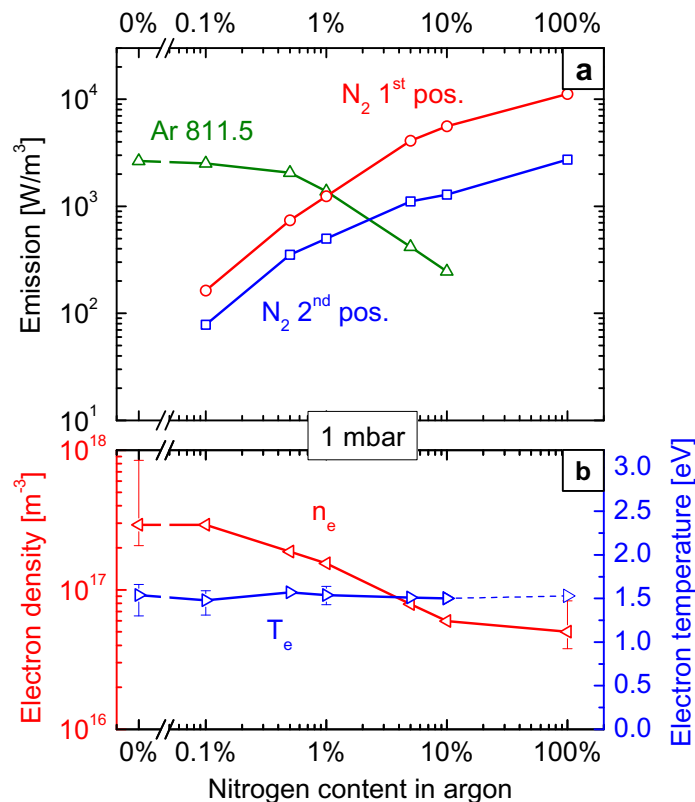


**Figure 4.** Dependence of (a) the emission from nitrogen and argon and (b) the plasma parameters  $n_e$  and  $T_e$  on the nitrogen content for 1 mbar absolute pressure and a discharge current of 300 mA.

absolute pressure of 5 mbar (at 1% N<sub>2</sub> in Ar) the nitrogen emission is dominant (whereas the intensive argon line at 811.5 nm is still visible). In addition much more emission appears from the first positive system compared to the second positive system especially when keeping in mind that the total emission of the first positive system is roughly a factor of 5 more intense than the representative integral.

#### 4.2. Comparison with collisional radiative modelling

In a next step the CR model presented in section 3.2 was applied to calculate the population densities of the nitrogen states and thus the emission from the first and second positive systems using the known plasma parameters. This allows for a comparison to the measured radiation and for sensitivity studies. The latter is of high relevance to the identification of relevant excitation and de-excitation processes. In addition, calculations using a simple corona model are performed in order to highlight the need for a CR model. In this corona model, electron impact excitation (processes (2) and (3) in table 2) is balanced with spontaneous emission (reactions (9) and (10)) whereas cascading from the C to the B state via the second positive system is neglected as well in the balance for the B state.

Since the CR model is not vibrationally resolved the total emission of the transition systems is calculated. Therefore the measured fraction from the first positive system as it is integrated

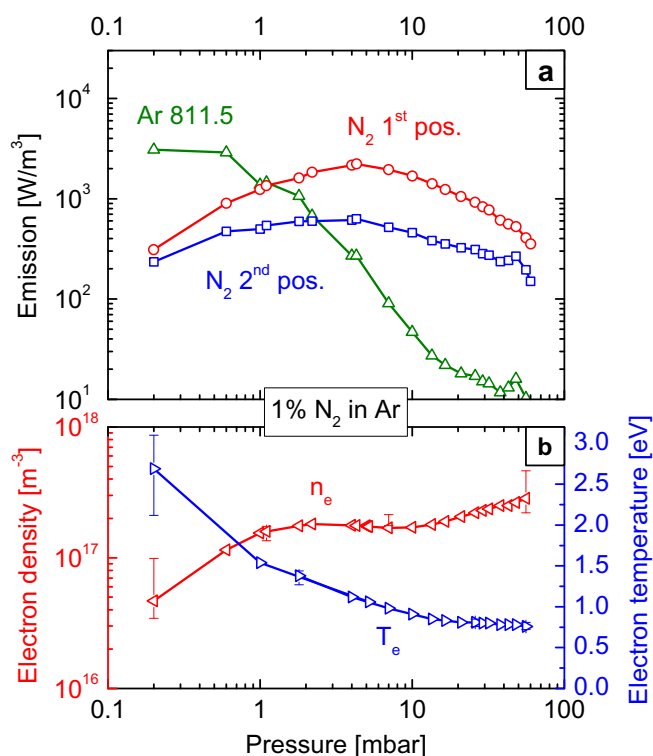


**Figure 5.** Pressure dependence of (a) the emission from nitrogen and argon and (b) the plasma parameters  $n_e$  and  $T_e$  for 1%  $\text{N}_2$  in argon at a discharge current of 300 mA.

after section 4.1 has to be upscaled to take sequences from  $\Delta v = -4, \dots, +2$  into account as well. The sequences  $\Delta v = +3$  and  $\Delta v = +4$  are detected vibrationally resolved. This means the vibrational bands  $(B, v') \rightarrow (A, v'')$  can be used to determine the population densities of the vibrational levels  $v' = 3, \dots, 12$  applying the appropriate transition probabilities  $A_{BA}^{v'v''}$  [36]. The density distribution of the vibrational states of the B state can be characterized by a vibrational temperature representing a Boltzmann distribution. This is fulfilled within the limits of  $\pm 10\%$  for the experimentally accessible vibrational levels, thus allowing for the calculation of the population densities of the non-accessible levels  $v' = 0, 1, 2$ . Together with the vibronic transition probabilities [36], the whole emission from this system can be calculated. Here the units of  $(\text{Ph}(\text{s} \cdot \text{m}^3)^{-1})$  are used instead of  $(\text{W} \text{m}^{-3})$  in section 4.1 as the vibrationally non-resolved CR model cannot take into account the photon energies of the individual emission bands.

**4.2.1. Pure nitrogen discharges.** Pure nitrogen discharges are investigated first, since influences from the background gas are excluded. In this case the standard  $T_e$ -diagnostic cannot be used as no argon emission occurs. However, the experimentally determined electron temperatures in nitrogen–argon plasmas at 1 mbar show independence from the gas mixture (see figure 4(b)), which is related to the similar ionization energies of the two gas species. Analogous behaviour is expected with varying pressure. Thus the modelling of pure nitrogen discharges was started with the pressure-dependent  $T_e$  value of nitrogen–argon plasmas (see figure 5(b)),

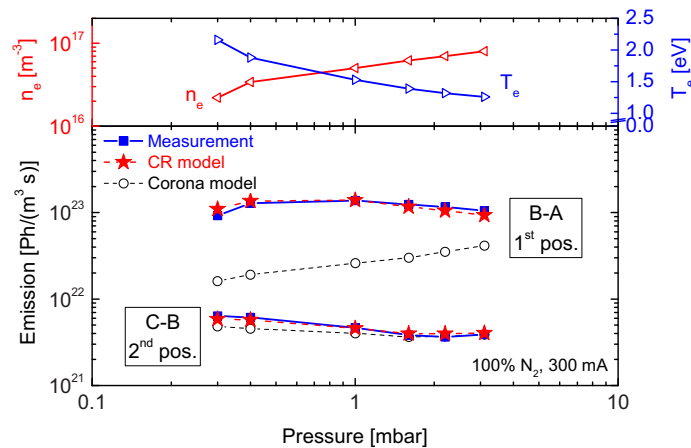


**Figure 6.** The measured and the calculated emission from the two nitrogen systems for pure nitrogen arc discharges together with the plasma parameters.

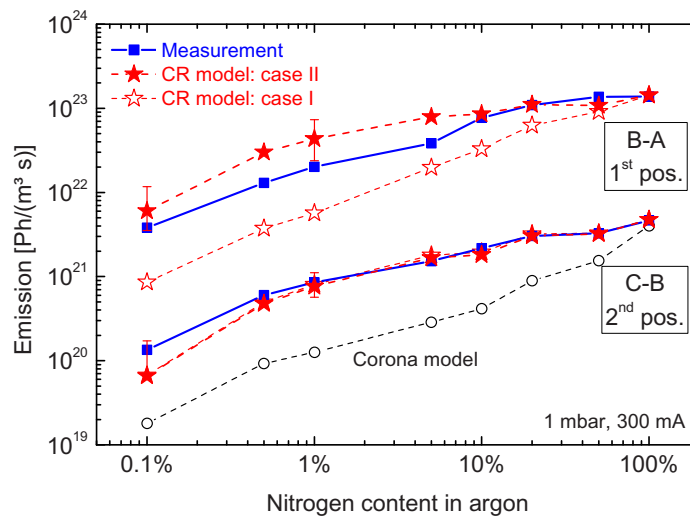
followed by an iterative adjustment of  $T_e$ . In each step, the CR calculated values for the emission are compared with the measured ones and subsequently  $T_e$  is re-adjusted serving as a new input parameter for another CR calculation. As expected, the variation in  $T_e$  by this iterative evaluation is very small.

Figure 6 shows the plasma parameters, the measured radiation and the calculated emission using the corona model and the CR model with varying absolute pressure between 0.3 and 3 mbar. The corona model clearly underestimates the emission of the first positive system, which demonstrates the relevance of further excitation channels besides electron impact from the ground state. For the C–B transition, satisfying agreement is observed using the corona model. However, the simulations with the CR model show a very precise reproduction of the measurements for both emission systems. This of course can at least partly be attributed to the recursive adjustment of  $T_e$  explained in the last paragraph. But nevertheless it shows the capability of the CR model to simulate the emission with appropriate plasma parameters. The different possible interpretations of reactions (16) and (17) (cases I and II) have no influence here due to the absence of argon in the discharge. A variation of the discharge current from 200 to 500 mA, which implies a variation of the electrical input power from 55 to 120 W, shows the same good agreement between measurement and simulation (not shown).

**4.2.2. Nitrogen–argon discharges.** Figure 7 shows the measured and the calculated emission from both the nitrogen systems with a reduction of the nitrogen content from pure nitrogen discharges to 0.1%  $N_2$  in the argon background. The results of the CR calculations are shown for both possibilities for reactions (16) and (17) (case I:  $M = N_2$ ; case II:  $M = N_2 + Ar$ ). Calculations using the simple corona model are only presented for the C state since the B state is severely underestimated anyway (cf figure 6). For the input parameters  $n_e$  and  $T_e$  the values presented in figure 4(b) are taken.

With decreasing nitrogen content the underestimation of the C state by the corona model increases strongly, which indicates an excitation mechanism of the state  $N_2 C^3\Pi_u$  via argon. However, the CR calculations reproduce very well the measured emission from the second positive system. This can be clearly attributed to the well-known excitation transfer





**Figure 7.** The measured and the calculated emission from the two nitrogen systems for nitrogen–argon mixtures at an absolute pressure of 1 mbar. For the CR model the results for the two cases are shown (see text), and for the C–B transition the corona results are also shown.

from the metastable argon states  $1s_5$  and  $1s_3$  (reaction (18)). On the other hand, the emission from the C–B transition is not sensitive to the case study.

The first positive system, however, shows a high sensitivity to the different interpretations of the transitions between the A state and the B state, i.e. the case study, in particular at high argon contents. Agreement with the measurements can be achieved only if processes (16) and (17) are treated as collision-induced crossings within one nitrogen molecule where the collision partner can be either a nitrogen molecule or an argon atom (case II). With these results, the excitation transfer perception suggested by Piper or Pravilov [46, 47] (case I) seems to become less important in favour of the collisional transfer approach [48–51].

The dependences on absolute pressure are shown in figure 8 for a nitrogen content of 1% in argon. Again CR calculations of both alternatives for reactions (16) and (17) are presented, having a great influence on the B state. Apart from pressures beyond 5 mbar the calculated emission for case II is in good agreement with the measurements for both nitrogen systems, which again confirms the relevance of collision-induced transitions between the A state and the B state.

However, at high pressures the deviation between the calculation and the measurement increases for both systems. While for the C state the CR calculation can be brought into agreement with the measurement by just varying the input parameter  $T_e$  from 0.78 to 0.84 eV (which is within the error limits) the B state is still underestimated by this adaptation. In addition, it can be seen that at this high pressure of 48 mbar a very small variation of  $\Delta T_e = +0.06$  eV strongly influences the population densities of the radiating nitrogen states: a factor of 2 for the B state and a factor of 3 for the C state can be gained. Therefore, the modelling is very sensitive to the electron temperature but can, on the other hand, be used in future to determine  $T_e$  with high accuracy if the CR model is validated.

The strong sensitivity of the C state density to  $T_e$  can be explained by the excitation via metastable argon atoms (process (18)). A rise in  $T_e$  (from 0.78 to 0.84 eV) mainly increases the

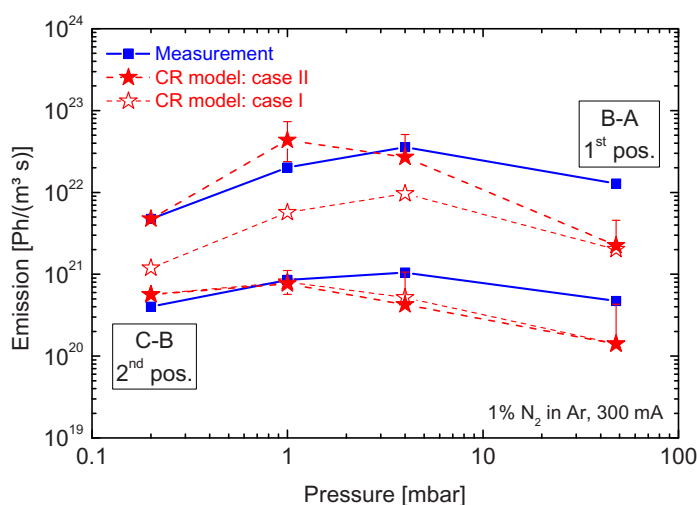


**Figure 8.** The measured and the calculated emission of the two nitrogen systems with varying absolute pressure at a nitrogen content of 1% in argon. For the CR model, the results for the two cases are shown (see text).

density of metastable argon atoms, in this case from  $8.5 \times 10^{14}$  to  $2.6 \times 10^{15} \text{ m}^{-3}$ , which is a factor of 3. This increased population of  $\text{Ar}_{\text{meta}}^*$  is directly transferred to the nitrogen C state via reaction (18), which results in enhanced emission from the second positive system by a factor of 3 again. Due to the extensive interactions between the B and the A states via reactions (4), (9), (12), (16) and (17) it is difficult to decide which processes lead to the enhanced emission from the first positive system. The CR calculations show that the populations of both states A and B increase roughly by a factor of 2 due to the variation in electron temperature by +0.06 eV.

Nevertheless, the reason for the difference between CR calculation and measurement in the first positive system is not yet clear. A crucial point at this high pressure might be the relevance of the vibrationally resolved quenching by argon, which is treated by a constant effective rate coefficient in reaction (20). This effective value is deduced from the vibrational population at 1 mbar. The vibrationally resolved quenching rate coefficients [44] are larger for higher vibrational quantum numbers. Together with an experimentally determined decrease of the vibrational temperature with rising pressure, it is obvious that quenching by argon is overestimated in the current CR model at high pressures. Another issue might be the relevance of further electronic states of nitrogen. As stated in section 3.2.5, many other levels can contribute to the energy exchange to or from the B state due to the proximity of their potential curves [50] and could therefore modify the population density. The quantitative influence of these aspects on the population of the B state is a major point for further investigations.

To summarize, case II of the two alternatives for the interpretation of reactions (16) and (17) reproduces the measured emission from the first positive system of nitrogen up to pressures of about 5 mbar, whereas the second positive system can be reproduced for absolute pressures from 0.2 to 50 mbar. Together with the corresponding results from the variation of the nitrogen content at 1 mbar the present CR model allows for discussion of the main excitation channels of the nitrogen systems for several orders of magnitude in nitrogen content and absolute pressure.

4.2.3. *Important processes.* By successively neglecting particular processes in the CR calculations, the following reactions have been identified as essential for the density of the excited nitrogen states and thus for the emission ('+' stands for excitation; '-' for de-excitation; numbers refer to the processes in table 2):

*Population of the state  $N_2$  B<sup>3</sup> $\Pi_g$*

- + Electron impact excitation from the ground state (2)
- +/- Collision-induced transitions involving the A state (16) and (17) whereas  $M = N_2 + Ar$
- Spontaneous emission: first positive system (9)
- Quenching by argon (20)

*Population of the state  $N_2$  C<sup>3</sup> $\Pi_u$*

- + Electron impact excitation from the ground state (3)
- + Energy pooling between metastable nitrogen molecules (13)
- + Excitation transfer from metastable argon atoms (18)
- Spontaneous emission: second positive system (10)

It has been observed that for the present  $N_2$ -Ar low-pressure arc discharges, the electron impact processes and spontaneous emission lose relevance with increasing argon content and increasing absolute pressure in favour of the heavy-particle reactions. The collision-induced transitions among the A and B states including the possibility of a crossing induced by argon atoms are substantial in the whole considered parameter space. Quenching of the nitrogen B state by argon atoms is most relevant at high pressures and high argon content. This leads to de-excitation of the B state at high pressures at the cost of radiation from the first positive system. For the C state the three main excitation channels, which are already well-known from the literature, interchange their importance when varying the discharge parameters, whereas the only relevant de-excitation mechanism is spontaneous emission forming the radiation of the second positive system. Due to the high relevance of energy transfer from metastable argon atoms, the C state is very sensitive to the density  $n_{Ar^*_{meta}}$ , which in turn strongly depends on the electron temperature.

#### 4.3. Radiation efficiencies and variation of the discharge current

In the presented parameter studies of varying nitrogen content and absolute pressure, the discharge current was kept constant at 300 mA. However, the gas composition of the low-pressure arc discharge strongly influences the electrical power consumption which is needed to sustain this discharge current (as shown in figure 9 for the pressure dependence). This has to be taken into account when assessing the emission with regard to the application as an efficient light source.

Therefore, radiation efficiencies of the discharges were investigated next. They are defined as the ratio of the electrical input power  $P_{el}$  to the emitted radiation power  $P_{rad}$ . As the CR model is not capable of calculating the required electrical input power and therefore cannot predict the radiation efficiencies, these values have to be determined experimentally. The electrical power is recorded by the power meter within the circuit taking into account the phase angle  $\cos(\Phi)$  between voltage and current, which is nearly unity as expected for arc discharges. For the radiation power the integral emission from the UV and the VIS spectral range is of relevance.

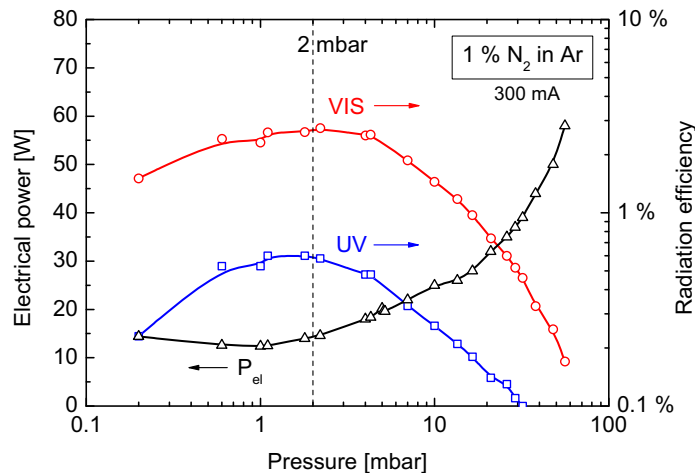


**Figure 9.** Pressure dependence of the electrical input power and the efficiencies for UV and VIS radiation in a gas mixture of 1% nitrogen in argon. The dashed line identifies the optimal absolute pressure.

Therefore the considered wavelength sections are 260–400 nm for the UV and 400–750 nm for the VIS emission. While the former exactly represents the second positive nitrogen system, the latter consists of parts from the first positive nitrogen system together with some argon emission lines.

To compare the different gas fillings regarding the radiation efficiency, first the optimal pressure for each nitrogen concentration was determined. In figure 9, the efficiencies in producing VIS and UV light together with the required electrical power for a nitrogen content of 1% in argon and a discharge current of 300 mA are shown. One can see a maximum in the efficiencies of 0.6% for UV and 2.7% for VIS radiation around 2 mbar where  $P_{el} = 14$  W.

Figure 10 summarizes these values for several nitrogen concentrations each at their optimal absolute pressure determined in the aforementioned way. An increase in the efficiency in producing UV and VIS radiation at higher contents of nitrogen can be observed. The maximum is reached for nitrogen concentrations of 5–10% in an argon background at 1 mbar absolute pressure: about 5% of the electrical input power can be emitted as useful radiation (UV and VIS spectral range).

As conventional fluorescent lamps with mercury have an efficiency in producing VIS light of about 25% (taking into account the conversion losses), a further enhancement of the nitrogen emission is envisaged to gain a factor of 4–5. This reveals the objective of ongoing investigations on nitrogen arc discharges for lighting purposes. Figure 10 suggests to investigate higher nitrogen contents for instance. In general, an increase in radiation efficiency can be achieved by enhancing the nitrogen emission since the line emission from the argon background plays only a minor role at  $N_2$  concentrations above 5% (see section 4.1). For this purpose the important excitation and de-excitation channels of the emitting nitrogen states identified by CR modelling (see section 4.2.3) can be used to determine possible improvements to the discharge.

An easy way to just intensify the emission is to increase the input power. This was done by varying the discharge current for a constant gas composition and the effect on the radiation efficiency was analysed. A variation between 100 and 500 mA results in a linear response of the parameters  $P_{el}$ ,  $P_{rad}$  and  $n_e$ , whereas the electron temperature remains constant. This means

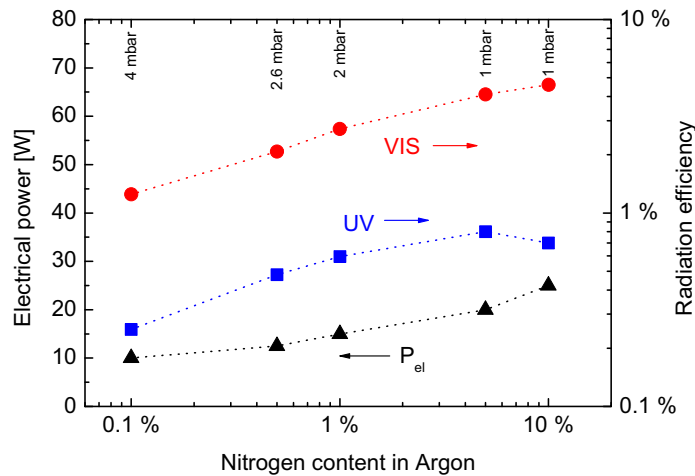


**Figure 10.** Radiation efficiency and required electrical power for the examined nitrogen concentrations at the corresponding optimal absolute pressures and a discharge current of 300 mA.

that the total radiation efficiency is not affected. However, this demonstrates the possibility for a simple way to dim the discharge.

## 5. Conclusions

To analyse the potential of a possible substitute for mercury in general lighting, nitrogen low-pressure arc discharges with argon as background buffer gas were investigated with an experimental setup close to conventional fluorescent lamps. Characterization of the nitrogen–argon discharges was done by means of optical emission spectroscopy for nitrogen contents of 0.1% to pure nitrogen, absolute pressures of 0.2–200 mbar and discharge currents between 100 and 500 mA.

The first positive system of nitrogen in the VIS range (starting from 500 nm) is very prominent in the spectra of such plasmas. Together with the conversion of the UV emission from the second positive system (260–430 nm) to fill the spectral gap in the blue, nitrogen arc discharges are very suitable for lighting purposes. The absolute intensity and efficiency of the nitrogen emission as well as the relative intensity among the two nitrogen systems strongly depend on the nitrogen content and the discharge pressure. The most efficient radiation so far is obtained at a gas filling with high concentrations of nitrogen in an argon background and a pressure of 1 mbar: 5% of VIS and 1% of UV efficiency can be reached. The optimal discharge parameters of gas mixture, pressure and current are ideal for direct usage in commercial fluorescent lamps and the investigated independence of the efficiency from variations of the discharge current provides an opportunity for easily dimming such a nitrogen-based lamp. However, the radiation efficiencies need to be further optimized in ongoing research efforts to compete with the well-established mercury-based lamps.

In order to identify the dominant population channels of the emitting electronic levels, a CR model for the states  $A^3\Sigma_u^+$ ,  $B^3\Pi_g$  and  $C^3\Pi_u$  of nitrogen was established. It revealed that heavy-particle collisions such as excitation transfer, collision-induced transitions and quenching have a significant influence across the investigated parameter space, in particular reactions

involving the background gas argon. As shown by the case study, the argon-induced collisional transition from the A state to the B state in nitrogen is an essential process for the excitation of the first positive system of nitrogen. In a next step, the model will be improved by vibrational resolution in order to solve remaining discrepancies and to get insight into the intricacies of the excitation and de-excitation channels.

Besides the investigation of higher nitrogen concentrations, a specific optimization of the discharge to enhance the N<sub>2</sub> emission could be the substitution of the background gas argon by another rare gas with lower quenching rate coefficients. This approach would also result in changing plasma parameters and in varying efficiency of the reactions of excitation transfer and collisional crossing, whose effects on the emission cannot be anticipated and need to be examined.

In summary, nitrogen low-pressure arc discharges have great potential as an environment-friendly, temperature-independent and easy-to-apply alternative in lamps for general lighting with a high potential to close the gap between today's mercury-based lamps and future LED lamps.

## Acknowledgments

The authors thank Dr Dirk Wunderlich from the Max-Planck-Institut für Plasmaphysik for his kind support in using the CR model Yacora and Florian Vogel from the Lehrstuhl für Experimentelle Plasmaphysik at the University of Augsburg for the provision of supplemental experimental data and the related fruitful discussions. This work was supported financially and scientifically by OSRAM AG Germany in Augsburg.

## References

- [1] Lister G G, Lawler J E, Lapatovich W P and Godyak V A 2004 *Rev. Mod. Phys.* **76** 541–98
- [2] Uhrlandt D, Bussiahn R, Gorchakov S, Lange H, Loffhagen D and Nötzold D 2005 *J. Phys. D: Appl. Phys.* **38** 3318–25
- [3] Robert E, Point S, Dozias S, Viladrosa R and Pouvesle J M 2010 *J. Phys. D: Appl. Phys.* **43** 135202
- [4] Kitsinelis S, Zissis G and Fokitis E 2009 *J. Phys. D: Appl. Phys.* **42** 045209
- [5] Jinno M, Takubo S, Hazata Y, Kitsinelis S and Motomura H 2005 *J. Phys. D: Appl. Phys.* **38** 3312–7
- [6] Kitsinelis S, Motomura H and Jinno M 2006 *J. Light Vis. Environ.* **30** 9–12
- [7] Sobolev N N 1989 *Electron-Excited Molecules in Nonequilibrium Plasma (Proc. Lebedev Physics Institute, Academy of Sciences of the USSR vol 179, supplemental vol 2)* (New York: Nova Science)
- [8] Behringer K 1991 *Plasma Phys. Control. Fusion* **33** 997–1028
- [9] Fantz U 2004 *Contrib. Plasma Phys.* **44** 508–15
- [10] Fantz U, Falter H, Franzen P, Wunderlich D, Berger M, Lorenz A, Kraus W, McNeely P, Riedl R and Speth E 2006 *Nucl. Fusion* **46** S297–306
- [11] Colli L and Facchini U 1952 *Rev. Sci. Instrum.* **23** 39–42
- [12] Kirshner J M and Toffolo D S 1952 *J. Appl. Phys.* **23** 594–8
- [13] Brown S C 1994 *Basic Data of Plasma Physics* (New York: AIP)
- [14] Ferreira C M and Loureiro J 1983 *J. Phys. D: Appl. Phys.* **16** 1611–21
- [15] Lisovskiy V, Booth J-P, Landry K, Douai D, Cassagne V and Yegorenkov V 2006 *J. Phys. D: Appl. Phys.* **39** 660–5
- [16] Jovanović J V, Basurto E, Sašić O, Hernández-Ávila J L, Petrović Z Lj and de Urquijo J 2009 *J. Phys. D: Appl. Phys.* **42** 045202

- [17] Long W H Jr, Bailey W F and Garscadden A 1976 *Phys. Rev. A* **13** 471–5
- [18] Vlček J 1989 *J. Phys. D: Appl. Phys.* **22** 623–31
- [19] Guimarães F and Bretagne J 1993 *Plasma Sources Sci. Technol.* **2** 127–37
- [20] Bogaerts A, Gijbels R and Vlček J 1998 *J. Appl. Phys.* **84** 121–36
- [21] Bultel A, van Ootegem B, Bourdon A and Vervisch P 2002 *Phys. Rev. E* **65** 046406
- [22] Zhu X and Pu Y 2007 *J. Phys. D: Appl. Phys.* **40** 2533–8
- [23] Wunderlich D, Dietrich S and Fantz U 2009 *J. Quant. Spectrosc. Radiat. Transfer* **110** 62–71
- [24] Dietrich S 2010 Verifikation von optischen Diagnostikmethoden an H<sub>2</sub>/D<sub>2</sub>-Plasmen *PhD Thesis* University of Augsburg
- [25] NIST 2011 *National Institute of Standard and Technologies* <http://physics.nist.gov>
- [26] Lofthus A and Krupenie P H 1977 *J. Phys. Chem. Ref. Data* **6** 113–307
- [27] Cicala G, De Tommaso E, Rainò A C, Lebedev Yu A and Shakhatov V A 2009 *Plasma Sources Sci. Technol.* **18** 025032
- [28] Bogaerts A 2009 *Spectrochim. Acta B* **64** 126–40
- [29] Debal F, Bretagne J, Jumet M, Wautelet M, Dauchot J P and Hecq M 1998 *Plasma Sources Sci. Technol.* **7** 219–29
- [30] Guerra V and Loureiro J 1997 *Plasma Sources Sci. Technol.* **6** 361–72
- [31] Kumar S and Ghosh P K 1993 *J. Phys. D: Appl. Phys.* **26** 1419–26
- [32] Nagpal R and Ghosh P K 1990 *J. Phys. D: Appl. Phys.* **23** 1663–70
- [33] Tabata T, Shirai T, Sataka M and Kubo H 2006 *At. Data Nucl. Data Tables* **92** 375–406
- [34] Biloiu C, Scime E E, Biloiu I A and Sun X 2007 *J. Appl. Phys.* **102** 053303
- [35] Freund R S, Wetzel R C and Shul R J 1990 *Phys. Rev. A* **41** 5861–8
- [36] Gilmore F R, Laher R R and Espy P J 1992 *J. Phys. Chem. Data* **21** 1005–107
- [37] Herzberg G 1953 *Molecular Spectra and Molecular Structure: I. Spectra of Diatomic Molecules* 2nd edn (New York: Van Nostrand)
- [38] Möller W 1993 *Appl. Phys. A* **56** 527–46
- [39] Piper L G 1988 *J. Chem. Phys.* **88** 6911–21
- [40] Piper L G 1988 *J. Chem. Phys.* **88** 231–9
- [41] Carr T W and Dondes S 1977 *J. Phys. Chem.* **81** 2225–8
- [42] Vredenburg E J D, Boom W, van Gerwen R J F and Beijerinck H C W 1990 *Chem. Phys.* **145** 267–91
- [43] Piper L G 1989 *J. Chem. Phys.* **90** 7087–95
- [44] Ricard A, Tétreault J and Hubert J 1991 *J. Phys. B: At. Mol. Opt. Phys.* **24** 1115–23
- [45] Calledé G, Deschamps J, Godart J L and Ricard A 1991 *J. Phys. D: Appl. Phys.* **24** 909–14
- [46] Piper L G 1989 *J. Chem. Phys.* **91** 864–73
- [47] Pravilov A M, Smirnova L G and Vilesov A F 1988 *Chem. Phys. Lett.* **144** 469–72
- [48] Campbell I M and Thrush B A 1967 *Proc. R. Soc. A* **296** 201–21
- [49] Gartner E M and Thrush B A 1975 *Proc. R. Soc. A* **346** 121–37
- [50] Carlson T A, Djurić N, Eрман P and Larsson M 1979 *Phys. Scr.* **19** 25–8
- [51] Bachmann R, Li X, Ottinger Ch and Vilesov A F 1992 *J. Chem. Phys.* **96** 5151–64
- [52] Cernogora G, Hochard L, Touzeau M and Ferreira C M 1981 *J. Phys. B: At. Mol. Phys.* **14** 2977–87